Engineering Applications of Artificial Intelligence xx (xxxx) xxxx–xxxx

Contents lists available at ScienceDirect

Engineering Applications of Artificial Intelligence

journal homepage: www.elsevier.com/locate/engappai

A spatially heterogeneous Gillespie algorithm modeling framework that enables individual molecule history and tracking

Justin Melunis, Uri Hershberg*

School of Biomedical Engineering and Health Sciences, Drexel University, 3141 Chestnut St., Philadelphia, PA 19104, United States

ARTICLE INFO

Keywords:
Integrated Particle System
Stochastic Modeling
Gillespie algorithm
Tracking
Immunology
STIM

ABSTRACT

Stochastic models allow investigators to simulate reactions in a discrete way that can account for fluctuations that are otherwise ignored within a deterministic approach. Integrated particle system (IPS) models are a form of stochastic model that take spatial distributions, environmental factors, and agent migration into consideration. Unlike agent based models (ABM), IPS models only rely on a set of general reactions to describe the interactions of molecules/entities, allowing for an easy cause-effect connection between macroscopic phenomena and microscopic behavior. However, IPS models currently do not track individual agents or apply manipulations to individual agent behavior based on their specific location or their individual history. Therefore, IPS models cannot incorporate agent-based manipulations and tracking while still relying on a set of basic assumptions that are needed to easily connect emergent phenomena to simplistic microscopic behaviors. Here we propose an IPS modeling framework where we convert the exact Gillespie algorithm into a 2 dimensional lattice space that allows for environmental factors where molecules can move stochastically, generating an overall heterogeneous molecule distribution. Individual molecules can be tracked without describing the rules of interaction for each specific individual molecule, forming a tracked IPS (TIPS) modeling framework. However, since each individual molecule is tagged, agent-based manipulations and the ability to alter agent behavior due to history can be incorporated into TIPS, allowing one to model biological systems that would otherwise have to rely on a pure ABM. We apply the TIPS modeling framework to STIM1(stromal interaction molecule 1)-Orai1(calcium release-activated calcium channel protein 1) binding and motion, in T cells as a result of T cell receptor activation a key component of the calcium response within lymphocytes that leads to the adaptive response of T cells in an immune response. Within this biological setting we show that observed patterns of reduced motion following activation can be explained by a diffusion trap coming from changes in the environment of interaction without any real change in the molecules movement rates.

1. Introduction

The Gillespie algorithm is a commonly used stochastic modeling framework that allows investigators to simulate reactions in a discrete way. This approach allows investigators to develop a model that can account for fluctuations that are otherwise ignored within a deterministic approach (Gillespie, 1977). However, the exact Gillespie algorithm approach assumes all reactions occur between evenly distributed entities/molecules in a well-mixed solution. In certain cases, such as predator-prey models, both spatial distributions and component migration play a large role in the predicted outcome. In these cases, rare events can emerge from the heterogeneity of the environment and individualized migration (Zelnik et al., 2015). In these cases an interacting particle system (IPS) model can allow for a spatially stochastic model to be able to easily incorporate the heterogeneous mixing of agents within the model as well as environmental dependencies by allowing discrete agents within the model to interact locally and migrate between patches that are spatially connected. These models rely on only basic assumptions and thus can retrace complex phenomena to basic components (Behar et al., 2014; Shnerb et al., 2000; Zion et al., 2010). This differs from agent based models (ABM) which describe each particular agent separately, making the model much more computationally intensive and the cause-effect connection of emergent events much more difficult to understand and quantify (Black and McKane, 2012).

However, IPS models look exclusively at population dynamics and cannot detail the path or history of an individual agent within that model. As the ability to image and track individual molecules increases so does the benefit of modeling frameworks that allows one to explicitly track each molecule in a model rise. Tracking individual molecules in

* Corresponding author.
E-mail addresses: Jdm347@drexel.edu (J. Melunis), uh25@drexel.edu (U. Hershberg).

http://dx.doi.org/10.1016/j.engappai.2016.09.010
Received 11 January 2016; Received in revised form 11 September 2016; Accepted 27 September 2016
Available online xxxx
0952-1976/

the model (and not just the data) becomes especially important if we want to tease out if environmental effects or individual changes in dynamics and interactions are the root cause for differences in motion of molecules we observe experimentally within the system. Furthermore, in such a model we can incorporate the impact of an entities history on its potential for action and motion. Something which clearly impacts many biological behaviors (Alam et al., 1996; Busch et al., 1998; Jameson et al., 1995).

1.1. Modeling scheme

Here we present a modeling framework that utilizes the exact spatial Gillespie algorithm binned into a 2 dimensional lattice space where molecules can move stochastically between bins generating an overall heterogeneous molecule distribution IPS. Our modeling scheme hinges around storing molecular information within hierarchical structure arrays. Molecules that are tracked, rely on history, or that have non-uniform rate distributions are individually tagged with a unique number. Tracking the individual molecules enables us to (1) track individual molecular location, form, and interactions during our simulation, and (2) store the interaction and history of the component molecules that make up molecular complexes. By creating a model that behaves as an IPS model while tracking individual molecule locations in a way consistent with how we image these molecules experimentally, we provide a distinct way to not only validate the dynamics of motion within the model, but to also a way to predict how the alteration of these dynamics would affect how we would observe motion within the system experimentally. Furthermore, the ability to incorporate in a stochastic simulation some aspects of an ABM, such as site dependent differences in individual agent rates or the ability to alter an individual agent's dynamics due to the history of the agent, provides a novel framework for modeling a multitude of biological systems in which we can provide a minimal set of assumptions while still incorporating many aspects of an ABM. By doing so, we hope to create a computationally friendly framework in which a model can be looked at for both individual and population dynamics while still allowing for an easy connection between the emergent phenomena and the underlying molecular dynamics.

1.2. Immunological example

Calcium is utilized as a secondary messenger signal in many adaptive cellular dynamics (Feske, 2007; Hogan et al., 2010; Stiber and Rosenberg, 2011). Recent studies have suggested that calcium plays a large role in immune cell differentiation, maturation and response to T cell receptor (TCR) signaling (Oh-hora et al., 2013). Cells actively move calcium both into the Endoplasmic Reticulum (ER) and out of the cell through the Plasma membrane (PM) to maintain a strong gradient to allow for effective signaling. In T cells, antigen-binding leads to the release of internal stores of calcium from the ER (Lewis, 2001). The loss of calcium within the ER releases STIMs, which dimerize and localize at the ER/PM junction, where they bind and activate Orai (Liou et al., 2007; Luik et al., 2008; Stathopulos et al., 2006; Stathopulos et al., 2013; Wu et al., 2006). Activated Orai channels become permeable to calcium, causing a flux of calcium to move across the membrane. Recent research has suggested that STIM and Orai may actually move in a non-directed fashion and that this localization may be due to the normal outcome of diffusion like movement near an obstruction, known as a diffusion trap (Kilch et al., 2013; Wu et al., 2006, 2014).

Here we apply our TIPS modeling framework to STIM1-Orai1 molecular interactions utilizing experimentally derived rates of reaction (Kilch et al., 2013). We utilize our novel technique of tracking our simulated stochastic model, allowing us to simulate how particles within our model would be observed during single particle tracking experiments. We show that this framework can help us to model a system of many agents (> 1000) while being able to distinguish the location and history in individual ones. We simulated a range of experiments, to try and distinguish the causes for the alteration in diffusion rates, of STIM1 molecules pre and post ER calcium release observed in previous single particle tracking experiments (Wu et al., 2014). We found that the observed changes in STIM and Orai1 motion following TCR activation can indeed be described without any recourse to localizing signals or changes in rates of motion. Rather, they appear to arise simply from the localization of STIM1 motion to the ER/PM junction following the binding of Orai1 (Luik et al., 2008; Wu et al., 2006, 2014).

2. Methods

2.1. Modeling framework

In order to create our modeling framework, we utilized the exact Gillespie algorithm (Gillespie, 1977). We separated our modeling environment into an m by n binned 2-d space in which each bin represents a square area in which we considered molecules to be well mixed within. We structured our framework to allow molecules to move from bin to bin based off the bin size, the molecules rate of motion, and environmental factors allowing for heterogeneous mixing (Kilch et al., 2013).

The exact Gillespie algorithm utilizes a random number generator to choose the next event to occur based on the probability of each event's occurrence. The probability of a reaction event between two molecules combining, R_u, occurring within the next time interval, dt, is calculated as the average probability that a particular combination of reactants inside volume, V, will react within the time interval, $c_u dt$, multiplied by the unique number of reactant combinations, h_u (Gillespie, 1977).

$$P(R_u)dt = c_u dt * h_u$$

c_u is known as the stochastic rate constant and is related to the deterministic reaction rate constant, K_u, by the relationship:

$$c_u = k_u * V$$

Due to this, if we assume Maxwell-Boltzmann velocity distributions we can adjust the stochastic rate constant of a 2 molecule colliding reaction, c_u, within an individual bin, i, by a factor of the number of bins, N, which is equivalent to the inverse square of the bin's edge length (Gillespie et al., 2014).

$$c_{ui} = N * c_u$$

Reactions in which individual occurrences are independent of the volume, such as decomposition, are not adjusted based on bin size.

It is important to state that this adjustment does not affect the rate of occurrence of a homogenously mixed environment. If the environment is evenly mixed of the reactants, r_1 and r_2, than the overall rate that the reaction, R_u, will occur will remain constant, as each bin will contain $\frac{1}{N}$ the number of molecules within it and the probability that the event occurs within a single bin will be $\frac{1}{N}$ the overall rate that the event will occur.

$$P(R_{ui})dt = c_{ui} dt * h_{ui} = N * c_u dt * \frac{1}{N^2} * h_u = \frac{1}{N} * P(R_u)dt$$

However, when the molecules become heterogeneously distributed, the probability of an event to occur within a single bin will be dependent on the unique combinations of reactions within that bin and the overall probability of occurrence of an event, R_u, will differ from the homogeneous probability. Rates of reaction and motion can be specified at a bin by bin level, allowing for heterogeneity of rates of reaction/motion due to environmental factors. A more extreme example of changing rates of motion in a heterogeneous way is to create restricted areas of motion that are molecule specific.

Our modeling framework allows molecules to able to move between bins. Molecules are commonly modeled with diffusive movement. In two dimensional diffusion, a molecule of type u has mean squared displacement, $\langle X_u^2 \rangle$, that is equal to four times its rate of diffusion, D_u, times the time displaced, dt. If we consider the event of the movement of molecule type u, M_u, between bins of volume, V_{bin}, then we can set an average probability of movement in time dt as:

$$P(M_u)dt = \frac{4*D_u}{V_{bin}} dt*h_u = M_u dt*h_u$$

If the environment is split to only a single bin, movement cannot occur between bins and the model reduces to an exact Gillespie algorithm. As the environment is split into more bins, the environment becomes more continuous, better resembling nature. In a homogeneous environment, the number of bins does not affect the rate in which reactions occur globally. However, the rate in which agents move between bins is increased, making the split of the environment into more bins more computationally demanding. In order to simulate the occurrence of an event, the rate of occurrence is calculated for each possible event at each bin location based on the environment and the quantity of molecules, as described above. The choice of what event and where it occurs is chosen by a random number generator, weighted by the event's rate of occurrence. If an agent type within the reaction is tagged, a random number is used to choose which agent preforms the reaction. Another random number between 0 and 1, r, is generated to calculate tau, the time it takes for the chosen event to occur (Gillespie, 1977). This calculation is done by the formula:

$$tau = \left(\frac{Log(1/r)}{TotalRate} \right)$$

Rates within our simulations were updated only in the bins in which the reaction occurred or an agent moved to or from. We have provided a pseudo code of how a simulation would advance (Fig. 1)..

2.2. Hierarchical structure

Our model relies on storing the component makeup of molecular complexes in a hierarchical structure based on the rules of component reactions within the simulation. Each complex type is stored inside its own cell array. The most basic complex of a single molecule that is tagged is stored as the tag number within a cell, i.e. [1]. When this combines with another single molecule, the two molecules are removed from their individual cells and combined within a single cell representing a complex i.e. [1 2]. Each location within this cell is specific for a certain molecule or complex type, in which the number represents the tag of an individual molecule. If we were to combine this complex, [1 2], with another molecule, the behavior of the individual components would dictate the hierarchical structure that is formed. If either component tagged as 1 or 2 behave individually when combining, then the new combination remains on the same level as these components, i.e. [1 2 3]. However, if components 1 and 2 behave as a single component within the new complex then they move to a sub-level within the complex that is within a second cell, i.e. [[1 2] 3]. If this complex behaves as a single component within another complex, this would again be placed within its own cell, forming another level within the complex.

When a tagged complex type is chosen at a specific (x,y) location, an individual complex of that form from that location is chosen from its cell array at random. If the event is motion, the complex is moved from its current array into the array corresponding with its new bin.

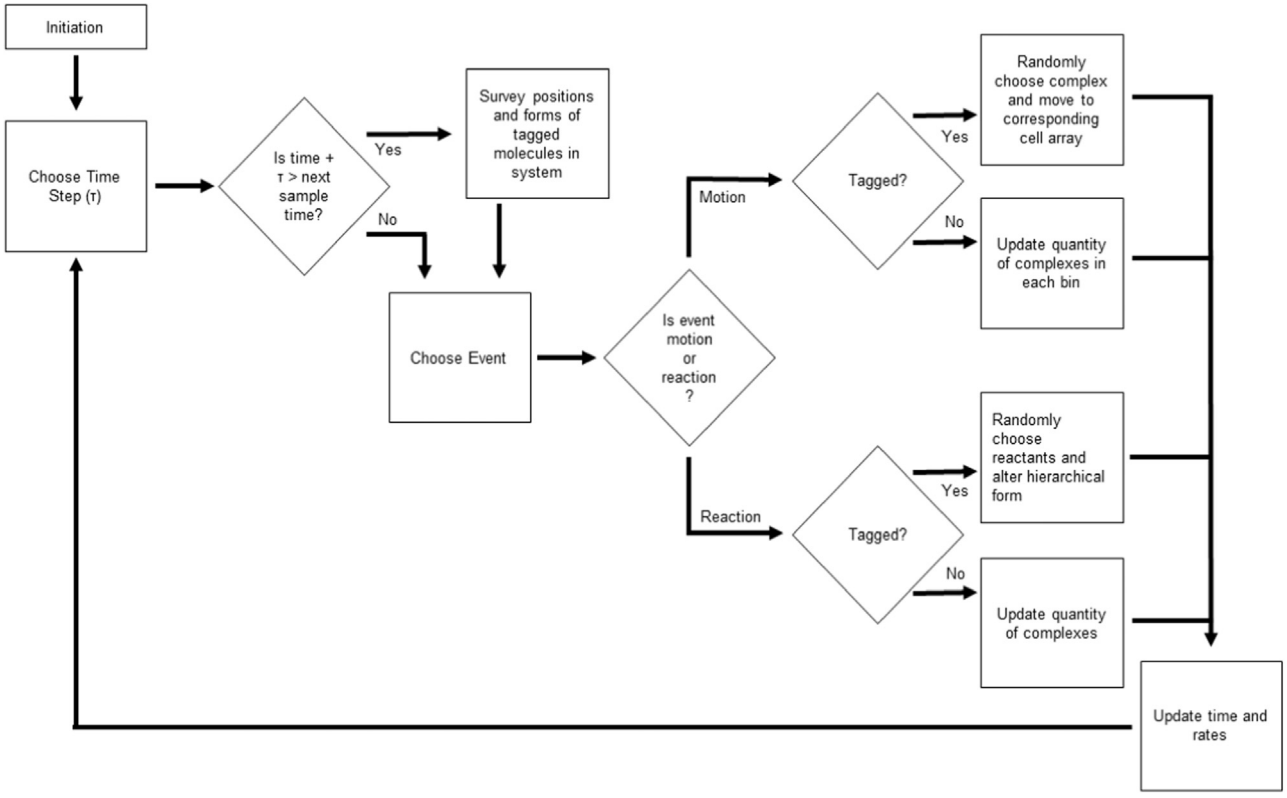

Fig. 1. Pseudo code of modeling framework. The simulation is initiated, placing molecules and calculating rates based on the position of molecules. A time step is chosen based on a random number and the overall rate of event occurrence. If this time step is greater than the next sample time, then the positions of all tagged molecules within the simulation are surveyed and recorded. Next an event is chosen. If the event is a motion event and the complex chosen to move is tagged, the specific complex chosen to be moved is chosen randomly and is moved to a cell array corresponding to the complex type and the new bin. If the complex chosen to move is not tagged, quantities are updated similar to an IPS modeling framework. If the event chosen is a reaction and tagged, the reactants are chosen at random and the form of the hierarchical structures of the molecular complexes are adjusted based on the type of reaction. The resultant complexes are then moved to their appropriate cell arrays. If any part of the interaction has a component that is not tagged, the quantity of that complex type is simply adjusted. All steps after the initiation are repeated until the end of the simulation.

Molecules which are not being tracked do not need to be tagged and instead just the number of molecules within a bin can be recorded. In these cases, the hierarchical form can simply not contain the non-tracked molecule's information and a change in form which contains a non-tracked agent being added or removed can be completed by adding or subtracting from the non-tracked agent's counter and then by moving the cell array in which the component is located within.

2.3. Agent-based manipulations, history and tracking

We can apply individualized agent reaction and movement rates into simulations using our modeling framework. To do so, a vector for each reaction that is agent dependent runs parallel to the cell array in which the agent's compositional information is stored. This vector dictates a value of scaling of the stochastic rate constant, c_{ui}. When we move the agent from its current cell array to another, either by motion or by a reaction, the scaling value is moved from its current vector to the vector corresponding to the new cell array. These values are used when updating the rate of occurrence of the reactions and when choosing the agent which reacts by weighing the random agent choice by the scaling values.

To track history and use it to influence rates of action, an array that stores values corresponding to historical events is generated, indexed by the molecular/complex tag. When an event occurs in which history effects a reaction, this array is updated and a transfer function is utilized to determine the new scaling factor for the event/events in which history effects. These values can record important interactions and implement them into individualized reaction rates, causing history to effect the future behavior of an individual molecule or a complex.

We created a simple model to show the implementation of individualized rates and history (Fig. 2)..

We incorporated the ability to track individual molecules within our spatial Gillespie algorithm by adding a numerical tag to each molecule that we wished to track. In order to be consistent with experimental data, the simulation space can be surveyed at intervals, similar to the rate of digital imaging in experimental tracking experiments. This process takes into consideration the hierarchical form and deconstructs it. The component locations within a complex are used to determine where tracked molecules are in space, time, and form. We have created functions in MATLAB to allow for a multitude of reactions and tracking that is available via our lab's GitHub on our lab's website (http://simlab.biomed.drexel.edu).

2.4. STIM/Orai implementation

STIM exists in the form of monomers, dimers, and in dimers conjugated with Orai (Kilch et al., 2013; Wu et al., 2014). In monomer or dimer form, STIM and Orai were free to move by random motion, but when conjugated to each other, they were restricted the ER-PM junction (the area of the ER and PM that are close enough to allow STIM-Orai interactions). STIM was able to bind to Orai in 4 states (OS1-OS4), representative of 1–4 STIM dimers bound to Orai. The binding of STIM dimers became within our model became less probable as more STIM dimers were bound to a specific Orai tetramer by a negative cooperatively factor of α (Fig. 3) (Hou et al., 2012; Kilch et al., 2013). To generate our simulation we considered STIM monomers and Orai monomers as being tagged. We set the reaction, R1, to combine two STIM monomers, S1 and S2, into a STIM dimer of form SD1=[S1, S2], and the reaction, R2, to reverse this combination. We considered a combination of an Orai molecule with dimers as OS1-OS4. When we combined one dimer with Orai, we created the hierarchical form OS1=[O1, SD1] =[O1, [S1, S2]]. The Orai molecule in our simulation was on the same hierarchical level as a STIM dimer, but that a STIM monomer was at a lower level, since the STIM dimer had to be removed from Orai before an individual monomer can be part of a reaction. Since our model called for the ability for any STIM dimer to be removed from OS2-OS4, STIM dimers behaved as independent components within the complex and remained on the same hierarchical level. Thus, we made OS2 of the form OS2=[[O1], [SD1], [SD2]] and so on. If we had a reaction in which OS2-OS4 was chosen to change into a STIM dimer and an Orai form with 1 less bound dimer, we chose a dimer at random to remove from the structure..

The space of the cell is simulated by a binned 2D space (Fig. 4). The environment was split between the general PM and the ER-PM junction. The area of simulation was set to be a 50 by 50 sized grid with each block being of an area of 0.01 μm^2 (length of .1 μm). The ER-PM junction was taken to be a 10 by 10 grid centered within the simulation space, in agreeance with the average puncta area that corresponded to the calculated edges of the diffusion trap observed by Wu, Covington, and Lewis (Wu et al., 2014)..

Our rates of diffusion were based off previously published research by Wu, Covington, and Lewis (Wu et al., 2014). The diffusion of a conjugant of molecules i and j is calculated by the formula:

$$\frac{1}{D_{ij}} = \frac{1}{D_i} + \frac{1}{D_j}$$

The 2-dimensional direction in which a molecule moved was chosen randomly between left, right, down, or up. When molecules move out of the field of view, a molecule corresponding to the molecule that left was produced coming in from the other side,

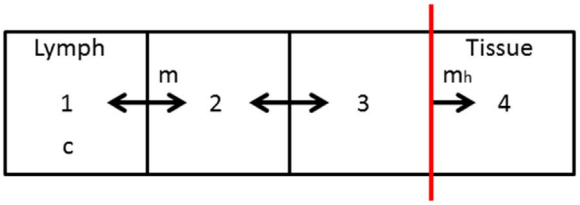

Fig. 2. A model of experienced immune cell motion to the tissue without the need for attractors. All immune cells started in bin 1. Antigen is uniformly spread across lymph compartments (1, 2, 3) and is not limiting. Individual binding rates, of Immune cells c, were set to a constant rate, C, multiplied by a scaling factor ranging from 1 to 100 at increments of 1. These agents moved between bins 1, 2, and 3 at a rate of m set to 1. Agents moved from bin 3 to bin 4 at a rate, m_h, which was dependent on the agent's history of binding. The scaling of m_h to m was set by the number of binding events that occurred, N_h, ranging from zero, if the specific cell had not undergone any binding, to *1* if the agent had undergone 5 or more binding events. The scaling factors were 0.0625, 0.125, 0.25, and 0.5 for 1–4 binding events respectfully.

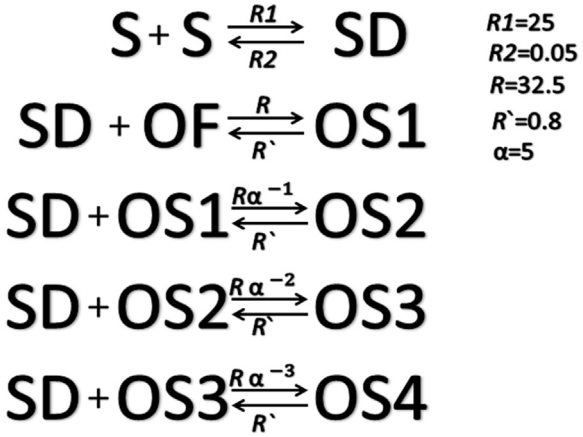

Fig. 3. Simulation Reactions. STIM (S), STIM dimer (SD), and Orai (which is either free (OF) or bound to up to 4 STIM dimers (OS1-OS4)). STIM monomers have a diffusion rate of 0.116 μm^2/s and free Orai have a diffusion rate of 0.09 μm^2/s. R1 and R2 represent the rates of STIM dimer on and off rates. R and R` represent the on and off rates of a STIM dimer with a free Orai with α representing the change in binding rates based on the conformation of the Orai conjugate.

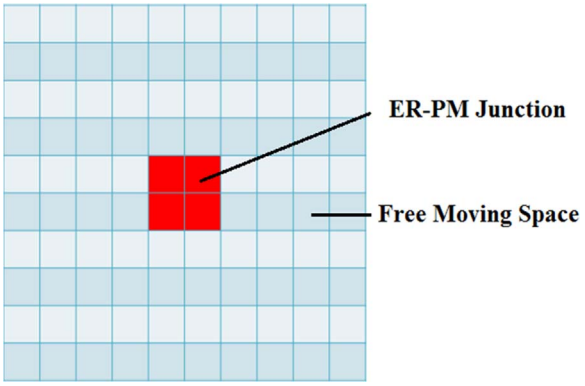

Fig. 4. Simulation Environment. Red represents the ER-PM junction where blue represents the local space surrounding the junction. Each box in the image represents a 5 by 5 set of boxes within the simulation.

making the simulation environment act as if it was continuous. However, the new molecule was marked with a new tag, so that we did not consider its location when analyzing the movement of the first molecule. This allowed us to maintain our count of molecules without causing errors within our tracking. In general, unless stated otherwise, our model followed the rates depicted in Kilch et al. Kilch et al., (2013).

With our model, we simulated 60 s time periods. First we allowed the STIM to equilibrate for 30 s and then we tracked it for another 30 s. Each simulation was of 1000 STIM molecules and 10 simulations were used per each initial condition. We analyzed individually monomer, dimer, and each conjugant's motion without the presence of interactions. We then looked at the motion in the presence of interactions with varying levels of Orai. When the simulation began molecules were randomly placed around the field of view and tagged with a number. At the set time interval of 0.1 s, their location and form were recorded, allowing us to track individual molecules. When estimating the current of calcium influx, we used the formula (Kilch et al., 2013; Hoover and Lewis, 2011; Li et al., 2011):

$$Icrac = 0.001 * OS1 + 0.025 * OS2 + 0.125 * OS3 + OS4$$

2.5. Diffusion analysis methods

We analyzed observed diffusion rates of individual molecules using tools from a previously published Monte Carlo method where the log of the displacement squared is compared to the log of time (O'Connor et al., 2011). We chose an observation time step of 0.1 s. For each simulation, we calculated the mean squared displacement as a function of time. $\langle r^2(t)\rangle$ represents the mean squared displacement for a time of t for an individual STIM molecule k. N is the number of STIM molecules that are observed for a time of t or longer. $X_k(t)$ is the two-dimensional position of the STIM molecule k at the time of t.

$$\langle r^2(t)\rangle = \frac{1}{N}\sum_{k=1}^{N} |X_k(t_o^k + t) - X_k(t_o^k)|^2$$

In 2-dimensional random motion, the displacement of molecule squared $\langle r^2(t)\rangle$ is equal to 4 times the rate of diffusion (D) multiplied by time (t).

$$\langle r^2(t)\rangle = 4Dt$$

Taking the natural logarithm of both sides of this equation yields:

$$\log(\langle r^2(t)\rangle) = \log(4D) + \log(t)$$

A weighted least-squared regression was utilized to find the slope of the logarithm of the mean squared displacement against the logarithm of time. The measurement of the logarithm of mean squared displacement was weighted according to the reciprocal of the logarithm of the displacement squared variance divided by its mean squared displacement, giving us a value for the variance of the logarithm of the mean squared displacement. We calculated these measurements for the first 1, 3, and 30 s of each simulation. We defined diffusive motion as a sample with a slope significantly greater than 0.9. For each data set, a t-test was used to calculate a p value for the hypothesis that the slope is equal to or greater than 0.9, which is representative of our definition of diffusive motion. This is because if motion is perfectly diffusive the slope should be 1. We further analyzed the observed diffusion rate based on 1-time step for individual molecule types. Here we took the mean displacement observed for 1-time step and divided it by 4 times the time step length.

We next calculated each molecule's diffusion individually. In this analysis we allowed for each step to be calculated as a new start time, t_o. For each individual STIM molecule in our simulation we calculated the mean squared displacement as a function of the time interval. By considering the displacement of each individual molecule, we allowed each calculable step size of size t to be considered an individual data point. Thus, the average mean squared displacement represents the average mean squared displacement for a step size of t over the entire observable time of the STIM molecule in question. When the amount of steps of size t, N, dropped below the arbitrary value of 5 data points we did not take the calculated mean displacement into consideration, and the STIM molecule was not taken into consideration if it was not observed in our simulation for at least 1 s (10 time steps). Furthermore, we limited our maximum time step to an arbitrary time step of 3 s (30 time steps). To calculate D of the individual molecule we considered a non-weighted least-squares regression of displacement and time. We then considered the value we would get for D if the individual molecule was moving diffusively. To do so, we fit the log of the displacement to the log of time with a fixed slope of 1. We took the fit intersection and divided by 4, due to our simulation being in 2-dimensions, and defined this as our observed diffusion rate. In this way we calculated an observed diffusion rate for every given molecule regardless of when we started observing it relative to its dispersal in the cell (the PM, the ER or the PM-ER junction).

3. Results

3.1. Individual molecule diffusion analysis

We ran simulations of individual molecule motion with and without the ability to interact. We considered free STIM motion to behave in a pre-antigen binding way where the ER Ca^{2+} stores are filled. We first analyzed all molecule types in isolation to determine how the boundaries of a diffusion trap would affect their ability to move. In order to calculate if movement of fixed state molecules were diffusive, for each time point we calculated the mean square displacement of STIM molecules from their initial location. To verify that in principle the molecules can create a diffusive pattern we expect we first looked at the mean square displacement of 1-time step for STIM molecules. We noticed that STIM forms not confined to the ER/PM junction fully matched the diffusion rates of their given value (Table 1). STIM in its Orai/STIM conjugate form showed a slight reduction in its diffusion.

We then calculated diffusion rates for time periods of 1,3, and 30 s and determined if it appeared to be diffusive or sub diffusive (as described in **Methods)**. We found that when analyzing diffusion over a short period of time (1 and 3 s), that STIM monomers and dimers both moved diffusively in our model and the rate of diffusion observed through our model was similar to their input diffusion rates (Table 1). Furthermore, this rate fit with the diffusion behavior of STIM1 in resting cells with depleted Ca2+ stores observed by Wu, Covington, and Lewis (Wu et al., 2014). As we observed longer time periods (30 s), STIM monomers looked to behave sub-diffusively. When we looked at STIM-Orai conjugates (OS1-OS4), their observed diffusion rate

Table 1
Population diffusion analysis of individual molecule types[a].

		1 Step	10 Steps (1 s)			30 Steps (3 s)			300 Steps (30 s)		
	Given D	D	Slope	Sub-diffusive	D	Slope	Sub-diffusive	D	Slope	Sub-diffusive	D
SF	0.116	0.116	0.999	No	0.113	0.983	No	0.110	0.858	Yes	0.098
SD	0.058	0.058	1.014	No	0.057	0.997	No	0.056	0.933	No	0.052
OS1	0.035	0.030	0.935	No	0.027	0.853	Yes	0.024	0.529	Yes	0.020
OS2	0.022	0.020	0.911	No	0.018	0.898	No	0.017	0.623	Yes	0.015
OS3	0.016	0.014	0.893	No	0.013	0.910	No	0.014	0.681	Yes	0.012
OS4	0.013	0.011	0.830	No	0.008	0.879	No	0.009	0.758	Yes	0.009

[a] D-The observed diffusion observed following 1,10, 30 and 300 time steps. Slope - the slope of the weighted least sum of squared linear fit of the natural logarithm of the displacement squared over the natural logarithm of time. Sub-Diffusive - Slope is significantly less than 0.9 by a *T*-test.

Table 2
Single molecule diffusion analysis[a].

Species	Mean D	Median D	STIM: Orai Ratio	Mean D	Median D
SF	0.110	0.109	**2:1**	0.045	0.045
SD	0.055	0.056	**5:1**	0.038	0.037
OS1	0.027	0.027	**8:1**	0.036	0.036
OS2	0.018	0.018	**10:1**	0.035	0.031
OS3	0.013	0.013	**20:1**	0.043	0.046
OS4	0.011	0.011			

[b] The mean and median observed diffusion rates of individual STIM molecule. The species correspond to the individual molecule diffusion analysis when these species act alone. STIM: Orai correspond to the full complement of interactions 30 s post-stimulation under varying ratios of STIM: Orai.

through our model was noticeably different from their input diffusion rates. At shorter periods of observed time (1–3 s), the conjugates motion bordered sub-diffusive motion and at longer time periods (30 s) all 4 conjugate forms behaved sub-diffusively. Next we calculated the diffusion rates of individual molecules using an altered monte-carlo technique (see **Methods** (O'Connor et al., 2011)). Our single molecule diffusion rates (Table 2) of individual molecule types showed similar mean and median rates of diffusion in comparison to the population dynamics over a duration of three seconds (Table 1).

3.2. Post-stimulation complex configuration and diffusion

We considered 5 different ratios of STIM and Orai abundance ranging from 2:1 to 20:1 STIM: Orai. We started STIM in the form of monomers and ran 10 simulations for each STIM: Orai ratio for 30 s post stimulation and depletion of calcium stores. At this point we looked at the configuration of molecules, the observed the number of STIM located at the ER-PM junction, and the estimated calcium current based on the molecular configuration of the STIM and Orai molecules. Our results showed that STIM became more highly bound to Orai in lower ratios of STIM: Orai (2:1, 5:1), but the Orai/STIM complexes stayed in configurations with less STIM (OS1, OS2). With higher ratios of STIM (8:1–20:1) more bound states were generated (OS4) (Fig. 5A). The lower ratios of STIM to Orai showed higher accumulation of STIM at the ER-PM junction (Fig. 5B). However, in our model, accumulation was not directly proportional to predicted calcium influx. If we accept the finding that Orai bound to more STIM dimmers conduct more calcium (Kilch et al., 2013; Hoover and Lewis, 2011; Li et al., 2011) then due to the ability to reach bound Orai states with a greater amount of bound STIM the optimal ratio in our simulation, optimizing maximal channel opening based on estimated relative calcium influx was roughly 8–10:1 STIM: Orai (Fig. 5C). These results agreed with the optimal ratio of 7.5:1 predicted by Kilch et al. model (Kilch et al., 2013). After 30 s of simulation, we allowed the simulation to go on for an additional 30 s, but tracked the locations of individual STIM molecules. We then calculated the STIM population slope, p value, and diffusion rates for the ratios of 2:1, 5:1, 8:1, 10:1, and 20:1 STIM: Orai for the next 1,3, and 30 s following the same procedure as we used to calculate the population's observed diffusion rates in the individual molecule diffusion analysis. Overall, we noticed that at short durations of diffusion (1–3 s), STIM did not look to show sub-diffusive motion (Table 3). However, the rate of STIM diffusion significantly drops in comparison to freely moving STIM monomers and dimers (Table 1). Furthermore, the rate of diffusion was lowest at a ratio of 8:1 STIM: Orai, where STIM has the highest number of maximally bound Orai. Our diffusion rates here were comparative to the reduced diffusion rates observed by Wu, Covington, and Lewis, in which they looked at STIM with and without the capability to bind to the PM without the presence of Orai (Wu et al., 2014). We also looked at individual molecule diffusion rates by calculating them in the same way we did in the individual molecule diffusion analysis. Our calculated median and mean diffusion rates of individual molecules showed that STIM moved the slowest at ratios of 8–10:1(Table 2), fitting to the observed population dynamics and the diffusion rates..

3.3. Performance characteristics

Our average run time for the STIM-Orai model for 30 simulated seconds at a ratio of 2:1 STIM to Orai was 1242.78 ± 42.76 s using a personal computer with an Intel® Core™ i7-4800MQ CPU @2.70 GHz and 24 GB of DDR3 1600 ram. The time of the simulation was mainly based on the motion of molecules and not the reaction between, as there was roughly 20 motion events per reaction event and the timing per event was similar regardless of type. The time per event increased as the number of molecules, N, in the simulation increased at a rate of N^1.08. This lead to roughly a 12-fold increase in simulation time with a 10-fold increase of molecule numbers. Currently, the main limitation is the ability to decrease bin size. The rate of molecule motion is inversely related to the square of a bin's edge length. Thus, a 10-fold decrease in bin edge length leads to roughly a 100-fold increase in the number of motion events within our simulation. We did not find evidence that the number of bins significantly altered the time per event within our simulation, and by design, the number of reaction events per simulation are independent of bin size.

4. Conclusions

We have created a novel form of IPS model that tracks individual molecules (TIPS). With this novel concept we can now follow a molecule even when it binds to other molecules, use its history to change its behavior and compare its dynamics to that observed in single molecule imaging experiments. Within the tracking, the population dynamics are not altered at all and the simulation reacts as if molecules were not being tracked. Due to this, the framework maintains the benefits of an IPS model while adding the benefit of being able to analyze individual molecule motion and interaction. However, this tracking comes at the cost of computation time. To save computation

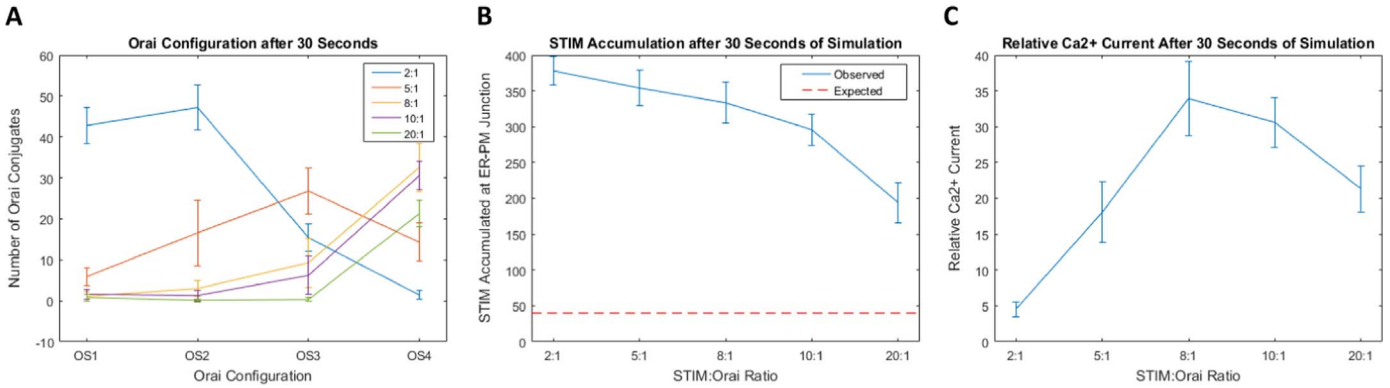

Fig. 5. A.The configuration of Orai conjugates after 30 s for each simulated STIM:Orai ratio. B. The number of STIM present after 30 s at the ER-PM junction. The red dotted line represents the expected number of STIM that would be present without any diffusive trap mechanisms. C. The calcium current relative to the maximal current of an individual channel based on Orai states after 30 s of simulation by the formula Icrac=0.001*OS1+0.025*OS2+0.125*OS3+OS4 [2]. Bars represent standard deviation.

Table 3
Population diffusion analysis of STIM at different times beyond 30 s post stimulation[a].

Ratio (S: O)	1 s			3 s			30 s		
	Slope	Sub-diffusive	D	Slope	Sub-diffusive	D	Slope	Sub-diffusive	D
2:1	0.986	No	0.047	0.956	No	0.044	0.824	Yes	0.040
5:1	0.956	No	0.039	0.955	No	0.039	0.780	Yes	0.033
8:1	0.935	No	0.037	0.903	No	0.035	0.794	Yes	0.032
10:1	0.977	No	0.041	0.956	No	0.040	0.785	Yes	0.034
20:1	0.951	No	0.045	0.928	No	0.043	0.845	Yes	0.041

[a] Diffusion is for all STIM molecules regardless of their conformation.

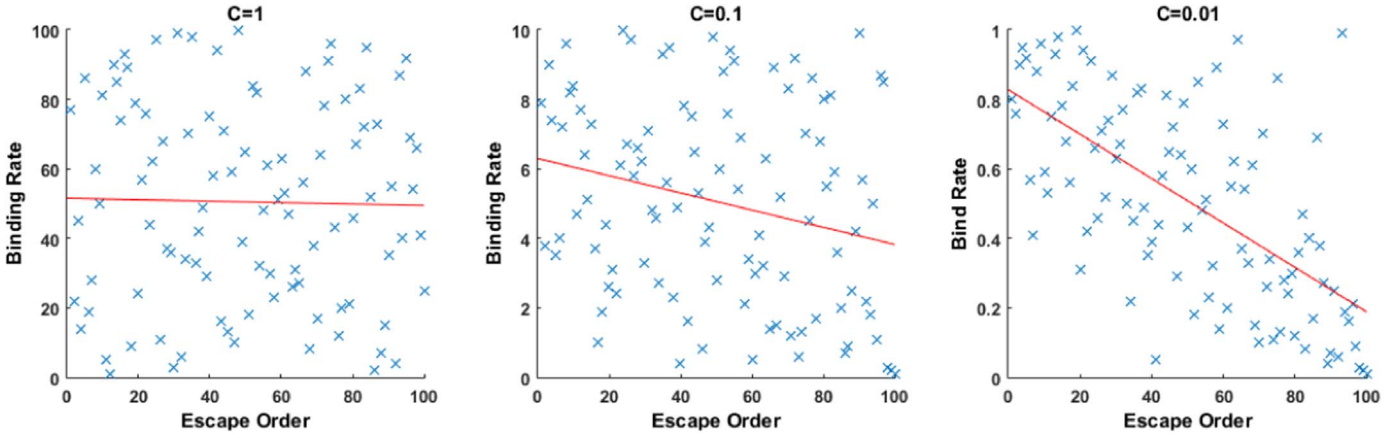

Fig. 6. History Simulation Results. The order in which immune cells escape to bin 4 was recorded for populations where the binding distribution was set by C equal to 1, 0.1, and 0.01 (subplots from left to right). A Pearson correlation and the corresponding p value were determined for the correlation of binding rates and escape orders. R values were 0.03, −0.25, and −0.60 with p values of $p > 0.75$, $p < 0.05$, and $p < 1e^{-10}$ respectfully. Each x in the figure represents an individual agent's escape order and binding rate. The red line is a least sum of squared fit of the data. This model shows that under certain conditions the ability to record history and apply it back into a simulation could drastically alter the outcome of a simulation. When C=1, the binding of immune cells to anitgen within the simulation happened much more rapidly. Most cells had a similar history of sufficient binding, making agents with different binding rates behave similarly. In a population with low binding rates (compared to the speed of motion) distinctions of binding rates became more meaningful in terms of thei individual cells history. Those cell's with a high binding rate interacted with more antigens and passed the barrier first.

time we allow tracking of only populations of interest and the ability to switch on and off the tracking of different molecule populations. Furthermore, we provide a way to add individualized reaction/motion rates, environmental factors, and history to this modeling framework (Fig. 6), allowing for the framework to fit a plethora of biological systems..

We applied our novel modeling framework to the tracking of STIM in a STIM/Orai iteration model. When we looked at diffusion, STIM monomers and dimers appeared to move diffusively near their input diffusion rate, while conjugates appeared to have sub-diffusive movements with a decreased diffusion rate. However, this was not due to some directed motion or alterations within the molecules/complexes themselves, but solely the result of being restricted to the boundary of the ER-PM junction. The combination of the boundary of the diffusion trap and the decrease in diffusion due to the formation of STIM-Orai conjugates decreased the population of STIM motion significantly enough to account fully for the observed differences of STIM motion pre and post ER calcium store release. Our model also allowed us to estimate the optimal ratio of STIM and Orai that would lead to maximal calcium influx. We observed that although higher Orai expression caused STIM to have a higher accumulation, this did not translate directly to higher calcium influx, as the channels may also be in less open states. Furthermore, too low levels of Orai expression lead to a shortage of Orai, which prevented calcium influx as well.

Therefore, in agreement with previous estimates (Kilch et al., 2013), we found that there is an optimal median range of STIM: Orai expression at a ratio of around 8:1 that should maximize calcium influx into the cell.

Acknowledgements

We would like to thank Dr. Bruce Freedman and Corbett Berry for their advice and conversations. Justin Melunis is recipient of the Department of Education Graduate Assistance in Areas of National Need (GAANN) Fellowship.

References

Alam, S.M., Travers, P.J., Wung, J.L., et al., 1996. T-cell-receptor affinity and thymocyte positive selection. Nature 381 (6583), 616–620. http://dx.doi.org/10.1038/381616a0.

Behar, H., Brenner, N., Louzoun, Y., 2014. Coexistence of productive and non-productive populations by fluctuation-driven spatio-temporal patterns. Theor. Popul. Biol. 96, 20–29. http://dx.doi.org/10.1016/j.tpb.2014.06.002.

Black, A.J., McKane, A.J., 2012. Stochastic formulation of ecological models and their applications. Trends Ecol. Evol. 27 (6), 337–345. http://dx.doi.org/10.1016/j.tree.2012.01.014.

Busch, D.H., Pilip, I., Pamer, E.G., 1998. Evolution of a complex TCR repertoire during primary and recall bacterial infection. J. Exp. Med. 188 (1), 61–70. http://dx.doi.org/10.1084/jem.188.1.61.

Feske, S., 2007. Calcium signaling in lymphocyte activation and disease. Nat. Rev. Immunol. 7, 690–702. http://dx.doi.org/10.1038/nri2152.

Gillespie, D., 1977. Exact stochastic simulation of coupled chemical reactions. Phys. Chem. 81 (25), 2340–2361. http://dx.doi.org/10.1021/j100540a008.

Gillespie, D.T., Petzold, L.R., Seitaridou, E., 2014. Validity conditions for stochastic chemical kinetics in diffusion-limited systems. J. Chem. Phys. 140 (5), 054111. http://dx.doi.org/10.1053/1.4863990.

Hogan, P.G., Lewis, R.S., Rao, A., 2010. Molecular basis of calcium signaling in lymphocytes: stim and ORAI. Annu Rev. Immunol. 28, 491–533. http://dx.doi.org/10.1146/annurev.immunol.021908.132550.

Hoover, P.J., Lewis, R.S., 2011. Stoichiometric requirements for trapping and gating of Ca2+ release-activated Ca2+(CRAC) channels by stromal interaction molecule 1 (STIM1). Proc. Natl. Acad. Sci. USA 108 (32), 13299–13304. http://dx.doi.org/10.1073/pnas.1101664108.

Hou, X., Pedi, L., Diver, M.M., Long, S.B., 2012. Crystal Structure of the Calcium Release-Activated Calcium Channel Orai. Science 338 (6112), 1308–1313. http://dx.doi.org/10.1126/science.1228757.

Jameson, S.C., Hogquist, K.A., Bevan, M.J., 1995. Positive selection of thymocytes. Annu Rev. Immunol. 13, 93–126.

Kilch, T., Alansary, D., Peglow, M., et al., 2013. Mutations of the Ca2+-sensing stromal interaction molecule STIM1 regulate Ca2+ influx by altered oligomerization of STIM1 and by destabilization of the Ca2+ Channel Orai1. J. Bio Chem. 288 (3), 1653–1664. http://dx.doi.org/10.1074/jbc.M112.417246.

Lewis, R.S., 2001. Calcium signaling mechanisms in T lymphocytes. Annu Rev. Immunol. 19, 497–521. http://dx.doi.org/10.1146/annurev.immunol.19.1.497.

Li, Z., Liu, L., Deng, Y., et al., 2011. Graded activation of CRAC channel by binding of different numbers of STIM1 to Orai1 subunits. Cell Res 21 (2), 305–315. http://dx.doi.org/10.1038/cr.2010.131.

Liou, J., Fivaz, M., Inoue, T., Meyer, T., 2007. Live-cell imaging reveals sequential oligomerization and local plasma membrane targeting of stromal interaction molecule 1 after Ca^{2+} store depletion. Proc. Natl. Acad. Sci. USA 104 (22), 9301–9306. http://dx.doi.org/10.1073/pnas.0702866104.

Luik, R.M., Wang, B., Prakriya, M., Wu, M.M., Lewis, R.S., 2008. Oligomerization of STIM1 couples ER calcium depletion to CRAC channel activation. Nature 454 (7203), 538–542. http://dx.doi.org/10.1038/nature07065.

Oh-hora, M., Komatsu, N., Pishyareh, M., et al., 2013. Agonist-selected T cell development requires strong T cell receptor signaling and store-operated calcium entry. Immunity 38 (5), 881–895. http://dx.doi.org/10.1016/j.immuni.2013.02.008.

O'Connor, M.J., Hauser, A.E., Haberman, A.M., Kleinstein, S.H., 2011. Activated germinal centre B cells undergo directed migration. Int J. Data Min. Bioinform 5 (3), 321–331. http://dx.doi.org/10.1504/IJDMB.2011.040387.

Shnerb, N.M., Louzoun, Y., Bettelheim, E., Solomon, S., 2000. The importance of being discrete: life always wins on the surface. Proc. Natl. Acad. Sci. U. S. A. 97 (19), 10322–10324. http://dx.doi.org/10.1073/pnas.180263697.

Stathopulos, P.B., Li, G.Y., Plevin, M.J., Ames, J.B., Ikura, M., 2006. Stored Ca^{2+} depletion-induced oligomerization of stromal interaction molecule 1 (STIM1) via the EF-SAM region: an initiation mechanism for capacitive Ca^{2+} entry. J. Biol. Chem. 281 (47), 35855–35862. http://dx.doi.org/10.1074/jbc.M608247200.

Stathopulos, P.B., Schindl, R., Fahrner, M., et al., 2013. STIM1/Orai1 coiled-coil interplay in the regulation of store-operated calcium entry. Nat. Commun. 4, 2963. http://dx.doi.org/10.1038/ncomms3963.

Stiber, J.A., Rosenberg, P.B., 2011. The role of store-operated calcium influx in skeletal muscle signaling. Cell Calcium 49 (5), 341–349. http://dx.doi.org/10.1016/j.ceca.2010.11.012.

Wu, M.M., Buchanan, J., Luik, R.M., Lewis, R.S., 2006. Ca^{2+} store depletion causes STIM1 to accumulate in ER regions closely associated with the plasma membrane. J. Cell Biol. 174 (6), 803–813. http://dx.doi.org/10.1083/jcb.200604014.

Wu, M.M., Covington, E.D., Lewis, R.S., 2014. Single-molecule analysis of diffusion and trapping of STIM1 and Orai1 at ER-plasma memreane junctions. Mol. Biol. Cell. 25 (22), 3672–3685. http://dx.doi.org/10.1091/mbc.E14-06-1107.

Zelnik, Y.R., Solomon, S., Yaari, G., 2015. Species survival emerge from rare events of individual migration. *Sci. Rep.* 5, 7877. http://dx.doi.org/10.1038/srep07877.

Zion, Y.B., Yaari, G., Shnerb, N.M., 2010. Optimizing metapopulation sustainability through a checkerboard strategy. PLoS Comput. Biol. 6 (1), e1000643. http://dx.doi.org/10.1371/journal.pcbi.1000643.